

CASO PRÁCTICO

Small inner marsh area delimitation using remote sensing spectral indexes and decision tree method in southern Brazil

Simioni, J. P. D.*¹, Guasselli, L. A.¹, Ruiz, L. F. C.¹, Nascimento, V. F.¹, de Oliveira, G.²

¹Federal University of Rio Grande do Sul, Center for Remote Sensing and Meteorology, Porto Alegre, Brazil.

²University of Kansas, Department of Geography and Atmospheric Science, Lawrence, KS, USA.

Abstract: Vast small inner marsh (SIM) areas have been lost in the past few decades through the conversion to agricultural, urban and industrial lands. The remaining marshes face several threats such as drainage for agriculture, construction of roads and port facilities, waste disposal, among others. This study integrates 17 remote sensing spectral indexes and decision tree (DT) method to map SIM areas using Sentinel 2A images from Summer and Winter seasons. Our results showed that remote sensing indexes, although not developed specifically for wetland delimitation, presented satisfactory results in order to classify these ecosystems. The indexes that showed to be more useful for marshes classification by DT techniques in the study area were NDTI, BI, NDPI and BI₂, with 25.9%, 17.7%, 11.1% and 0.8%, respectively. In general, the Proportion Correct (PC) found was 95.9% and 77.9% for the Summer and Winter images respectively. We hypothesize that this significant PC variation is related to the rice-planting period in the Summer and/or to the water level oscillation period in the Winter. For future studies, we recommend the use of active remote sensors (e.g., radar) and soil maps in addition to the remote sensing spectral indexes in order to obtain better results in the delimitation of small inner marsh areas.

Key words: marshes, Sentinel 2A, remote sensing, CART method.

Delimitación de pequeñas marismas interiores mediante índices espectrales y árboles de decisión en el sur de Brasil

Resumen: En las últimas décadas se han perdido grandes áreas de pequeñas marismas interiores (SIM) a través de la conversión a tierras agrícolas, urbanas e industriales. Las marismas restantes enfrentan varias amenazas, como el drenaje para la agricultura, la construcción de carreteras e instalaciones portuarias, la eliminación de residuos, entre otras. Este estudio integra 17 índices espectrales de teledetección y un método basado en árboles de decisión (DT) para cartografiar áreas de pequeñas marismas interiores utilizando imágenes del satélite Sentinel 2A de verano e invierno. Los resultados muestran que los índices de teledetección, aunque no han sido desarrollados específicamente para la delimitación de marismas, presentan resultados satisfactorios

To cite this article: Simioni, J. P. D., Guasselli, L. A., Ruiz, L. F. C., Nascimento, V. F., de Oliveira, G. 2018. Small inner marsh area delimitation using remote sensing spectral indexes and decision tree method in southern Brazil. *Revista de Teledetección*, 52, 55-66. <https://doi.org/10.4995/raet.2018.10366>

* Corresponding author: joao.delapasse@ufrgs.br

para clasificar estos ecosistemas. Los índices que demostraron ser más útiles para la clasificación de marismas mediante técnicas de DT en el área de estudio fueron el NDTI, BI, NDPI y BI₂, con 25.9%, 17.7%, 11.1% y 0.8%, respectivamente. En general, la proporción correcta encontrada fue de 95.9% y 77.9% para las imágenes de verano e invierno, respectivamente. Nuestra hipótesis es que esta variación significativa de la proporción correcta está relacionada con el período de siembra del arroz en verano y/o con el período de oscilación del nivel del agua en invierno. Para futuras investigaciones, recomendamos el uso de sensores remotos activos (por ejemplo, radar) y mapas de suelo además de los índices espectrales de teledetección para obtener mejores resultados en la delimitación de pequeñas áreas de marismas interiores.

Palabras clave: marismas, Sentinel 2A, teledetección, método CART.

1. Introduction

Marsh is a type of wetland (WL) characterized by the presence of hydromorphic soil, graminoids, aquatic vegetation, and shrubs or emergent plants adapted to flood pulses (Junk *et al.*, 1989; Visser and Sasser, 1999; Canadian Wetland Inventory Technical Group, 2016; Simioni *et al.*, 2017). The Environmental Protection Agency of the United States of America (USA) (2001) defines marshes as “often or continuously flooded wetlands characterized by emergent soft-stem vegetation adapted to saturated soil conditions”.

Vast small inner marsh (SIM) areas have been lost in the past few decades through the conversion to agricultural, urban and industrial lands (Gedan *et al.*, 2009). The remaining marshes face several threats such as drainage for agriculture, construction of roads and port facilities, waste disposal, among others (Liu *et al.*, 2013; Fluet-Chouinard *et al.*, 2015).

Yan *et al.* (2017) suggest that the classification of marsh areas is an important way to understand the spatio-temporal changes that they are submitted. Junk (2013); Junk *et al.* (2014); and Nunes da Cunha *et al.* (2015) argue that the delimitation is fundamental to manage, protect and maintain wetlands. Teixeira (2011) and Junk and Piedade (2015) point out that there are currently several data sources to delimitate large wetland areas. However, there are several difficulties for the delimitation of SIM areas, which have specific characteristics and dynamics (Junk *et al.*, 1989; Nunes da Cunha *et al.*, 2015; Mahdavi *et al.*, 2017).

In the early 2000's, the Ramsar Convention (2002) recommended the use of remote sensing (RS) and geoprocessing for wetlands classification, mapping, delimitation, and inventory (Artigas and

Yang, 2006; Judd *et al.*, 2007; Sharpe *et al.*, 2016; Dvoretz *et al.*, 2016). The radiometric, spectral and temporal resolutions of the satellites Landsat 5 and Landsat 8 and, recently, Sentinel 2A and 2B allow to conduct accurate studies for the identification of several types of wetlands (Jensen, 2007; Sharpe *et al.*, 2016; Kaplan and Avdan, 2017a).

Several authors have applied vegetation indexes (VIs) to delimitate, monitor and classify wetlands: 1) Stefano (2003) developed the water and wetland index (WWI) to identify different wetlands types; 2) Kulawardhana *et al.* (2007) used remote sensing indexes and digital elevation models to delimitate wetlands; 3) Sakané *et al.* (2011) classified, characterized and delimitated small wetlands using VIs; 4) Dong *et al.* (2014) applied NDVI (normalized difference vegetation index) and LSWI (land surface water index) for the mapping of lakes, rivers and flood plains; 5) White *et al.* (2016) adapted the NDVI to delimitate wetlands; 6) Kaplan and Avdan (2017a) used Sentinel 2A images to map wetlands using Sentinel 2A images; 7) Miranda *et al.* (2018) analyzed the vegetation variation in the Pantanal area in Brazil using VIs; and 8) Di Vittorio and Georgakakos (2018) used NDVI and MNDWI (Modified Normalized Difference Water Index) obtained from MODIS to map wetland areas.

In general, studies involving marshes focus on the characterization of salt or tidal marshes (Walsh *et al.*, 2014; Fariña *et al.*, 2017; Mcowen *et al.*, 2017; Mao *et al.*, 2018). These types of marsh have a grassy vegetation tolerant to salt water (Belluco *et al.*, 2006; Judd *et al.*, 2007) and have different water turbidity (Subramaniam and Saxena, 2011; Mondal and Bandyopadhyay, 2014) and soil types (Mao *et al.*, 2018) in comparison with inner marshes.

Based on the considerations above, this study proposes a method to delimitate SIM areas based on remote sensing spectral indexes and decision tree techniques using Sentinel 2A images.

1.1. Study Area

The study was conducted in the Banhado Grande (BG) marsh, located within the Gravataí river basin (GRB) in the eastern flank of Rio Grande do Sul State, Brazil (Figure 1).

As much of others Rio Grande do Sul marshes, the BG have historically suffered significant environmental impacts, such as drainage for agricultural crops (Belloli, 2016), soil erosion (Etchelar, 2017) and construction of roads (Silva, 2016).

The BG is a paludal environment with approximately 5951 ha (Ramos *et al.*, 2014). The main soil type found in the area is the gleisolo (Nielsen, 1994). The annual precipitation average varies between 1700 and 1800 mm (Rossato, 2011). In a study developed by Simioni *et al.* (2017) it was verified that in great flood periods it is established a connection between BG with Banhado dos Pachecos and Gravataí river floodplain. This connectivity is responsible for several interactions

between WLs, such as nutrients, sediments and organisms exchange.

According to Leite and Guasselli (2013) the BG vegetation patterns shows a seasonal variability regulated by flood pulses. During the dry season (Summer and Fall) there is a predominance of *cyperaceae* species while in the wet season (Winter and Spring) macrophytes and paludal vegetation prevails.

2. Material and Methods

2.1. Satellite Image Acquisition

In this study two Sentinel 2A images were used. Satellites Sentinel 2A and 2B are part of the Copernicus Program, which is managed by the European Community and European Space Agency (ESA). These satellites collect data on vegetation, soil moisture, as well as rivers and coastal areas. The images were obtained through Copernicus website (<https://scihub.copernicus.eu/>) in the level-1C for the bands 3 (green), 4 (red), 8 (NIR), 11 (SWIR 1) and 12 (SWIR 2) (Table 1). The images were obtained considering the dry and wet seasons in the region in order to evaluate the performance

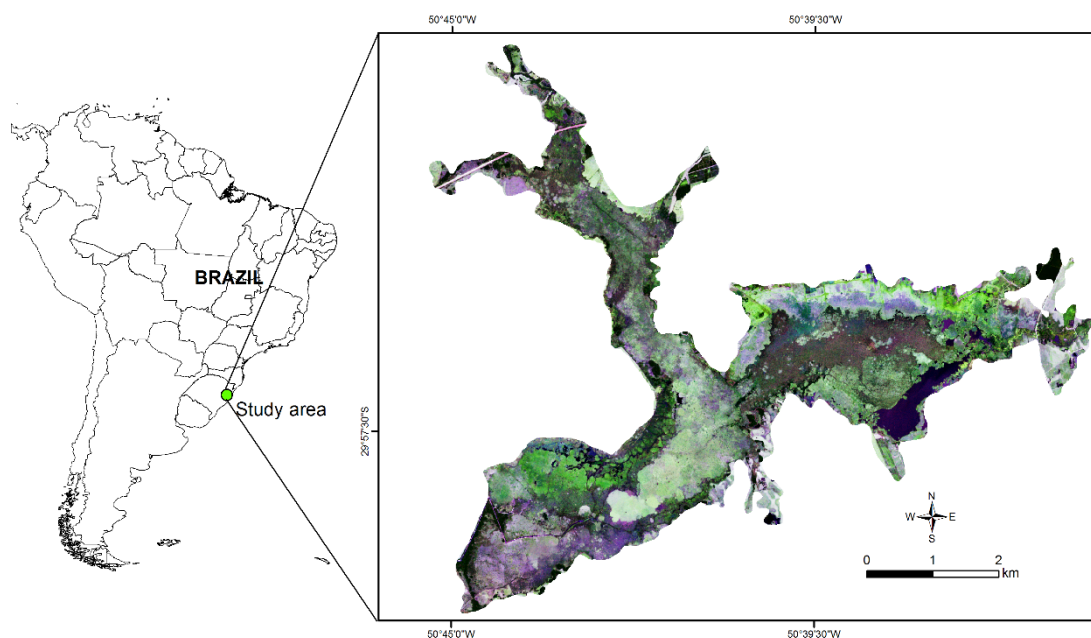


Figure 1. Map showing the location of the Banhado Grande marsh.

of the classification under two situations: 1) when the marsh surrounding areas are mainly used for rice cultivation (Summer and Fall); and 2) when there is higher amplitude of the water level oscillation (Winter and Spring).

Table 1. Sentinel 2A scenes used in the study.

Date	Sensor	Season	Level	Granule	Relative Orbit
02/09/2018	MSI	Summer	1C	T22JEM	038
07/19/2018	MSI	Winter	1C	T22JEM	038

First, the level-1C images were converted to surface reflectance using the *sen2cor* tool (Kaplan and Avdan, 2017b). The spatial resolution of the bands 3, 4, and 8 is 10 m while the spatial resolution of the bands 11 and 12 is 20 m. In this regard, we chose to resample the bands 11 (SWIR 1) and 12 (SWIR 2) to 10 m using the bilinear interpolation method according the proposition of Qianxiang et al. (2003).

2.2. Remote Sensing Spectral Indexes

We calculated seventeen vegetation, water and soil indexes using the Sentinel 2A images (Table 2). The indexes were applied using the ESA’s Sentinel Application Platform (SNAP) tool.

2.3. Samples

Using a WorldView-2 multispectral satellite image from 02/05/2018 with 1.85 m spatial resolution we selected 2000 random points for three different classes: 1) SIM; wet meadow (WM) and rice crops (RC). In order to align the geometric resolution between the WorldView-2 and Sentinel 2A images we used the Erdas Autosync Workstation tool.

We chose to collect samples for WM and RC because of the similarity of the plants spectral response during the growing season. Although BG has aquatic plants in both permanent and periodic flooding periods, no samples were collected for the apparent optical properties of the water since there are several remote sensing indexes for this purpose in literature.

Table 2. Remote sensing spectral indexes used in the study.

Index	Equation	Author (s)
Weighted Difference Vegetation Index	$WDVI = B8 - g \times B4$	(Clevers et al., 1989)
Soil Adjusted Vegetation Index	$SAVI = \frac{(1 + L) \times (B8 - B4)}{(B8 + B4 + L)}$	(Huete, 1988)
Transformed Normalized Difference Vegetation Index	$TNDVI = \sqrt{(NDVI + 0.5)}$	(Deering, 1975)
Brightness Index	$BI = \sqrt{\frac{(2 \times B4) + (2 \times B3)}{2}}$	(Escadafal, 1989)
Brightness Index_2	$BI_2 = \sqrt{\frac{(2 \times B4) + (2 \times B3) + (2 \times B8)}{3}}$	(Escadafal, 1989)
Ratio Vegetation Index	$RVI = B4/B8$	(Pearson & Miller, 1972)
Normalized Difference Water Index	$NDWI = (B8 - B11)/(B8 + B11)$	(Gao, 1996)
Normalized Difference Water Index 2	$NDWI_2 = (B3 - B8)/(B3 + B8)$	(McFeeters, 1996)
Normalized Difference Vegetation Index	$NDVI = (B8 - B4)/(B8 + B4)$	(Rouse et al., 1973)
Normalized Difference Turbidity Index	$NDTI = (B4 - B3)/(B4 + B3)$	(Lacaux et al., 2007)
Normalized Difference Pond Index	$NDPI = (B3 - B11 \times B12)/(B3 + B11 \times B12)$	(Lacaux et al., 2007)
Normalized Difference Index	$NDI45 = (B5 - B4)/(B5 + B4)$	(Delegido et al., 2011)
Modified Soil Adjusted Vegetation Index	$MSAVI = \frac{(1 + L) \times (B8 - B4)}{(B8 + B4 + L)}$	(Qi et al., 1994)
Modified Normalized Difference Water Index	$MNDWI = (B3 - B11)/(B3 + B11)$	(Xu, 2006)
Green Normalized Difference Vegetation Index	$GNDVI = (B8 - B3)/(B8 + B3)$	(Gitelson et al., 1996)
Difference Vegetation Index	$DVI = (B8 - B4)$	(Richardson & Wiegand, 1977)
Atmospherically Resistant Vegetation Index	$ARVI = (B8 - rb)/(B8 + rb)$	(Kaufman et al., 1992)

Sampling points were divided into 70% of training samples and 30% of validation samples. To analyze the classification accuracy we used the proportion correct (PC) (Pontius and Millones, 2011), producer’s accuracy (PA), and user’s accuracy (UA) (Congalton, 1991).

2.4. Decision Tree and Marsh Delimitation

The classification and regression trees (CART) method was used to discriminate the different classes. The CART method uses non-parametric statistics without probabilistic assumptions, selecting the necessary variables automatically (Friedl and Brodley, 1997). The CART is a classification procedure that breaks a dataset into smaller subsets based on a test defined in each tree branch or node, resulting in a binary decision tree with more homogeneous and pure nodes. The decision tree (DT) is composed by an initial node (root), a set of internal nodes (divisions), and a set of terminal nodes (leaves). The purpose of constructing a DT is to reduce the nodes impurities and then obtain the input variables relevance (e.g., spectral indexes) (Ruiz *et al.*, 2014).

The DT complexity and its size can be controlled by the depth and the sample numbers in inner nodes. The DT complexity depth and child nodes number influence the proportion of correct pattern elements (Ruiz *et al.*, 2014). We tested six different DT depth values (5, 10, 15, 20, 25, and 30) and six child nodes numbers (20, 40, 60, 80, 100, and 120) in order to find the best fit for the study area. We used the Gini index to measure the impurity of the tree branches.

To delineate the marsh, the CART classification with the highest PC was converted into conditional tests and then spatialized. Subsequently, the majority filter (MF) was applied to replace cells based on the majority value of adjacent neighboring pixels for both classifications (Ruiz *et al.*, 2014).

3. Results

3.1. Maximum Tree Depth

The maximum tree depth controls the maximum number of growth levels below the root node and

the minimum case numbers rules the minimum node case numbers. The nodes that do not meet these criteria have no divisions. The minimum case values increase lean towards to produce trees with fewer nodes. The Figure 2 shows the PC into the CART method in relation to maximum tree depth and the minimum case numbers for the validation samples.

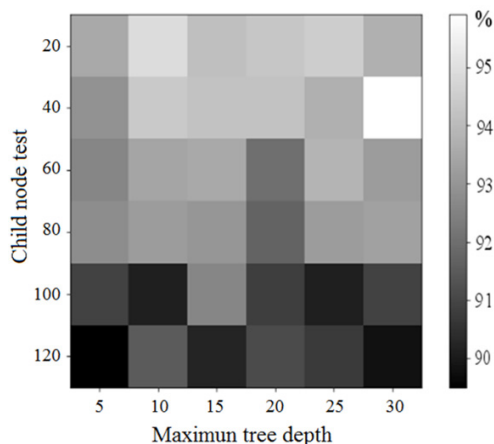


Figure 2. Decision tree (DT) proportion correct (PC) using the classification and regression trees (CART) method.

The highest PC was found at depths ranging from 20 to 30 and minimum cases between 20 and 40. The maximum depth of 30 and the minimum case numbers of 40 were the most accurate among all the parameters analyzed, achieving the PC of 95.9% for the validation samples during the Summer and 77.9% during the Winter images. It was observed a trend of reduction in the PC values when the minimum case numbers is greater than or equal to 100.

3.2. Decision Tree Classification

We used the same training samples to classify the Summer (02/09/2018) and Winter (07/19/2018) images. The DT classification was automatically divided into 18 nodes (Figure 3). The root node determined by the CART method was the NDTI (normalized difference turbidity index) (Lacaux *et al.*, 2007). The NDTI values lower than -0.31 corresponded to $\sim 5\%$ of the samples as SIM and they were directly related to ARVI (atmospherically resistant vegetation index) (Kaufman *et al.*, 1992). The NDTI and ARVI values showed

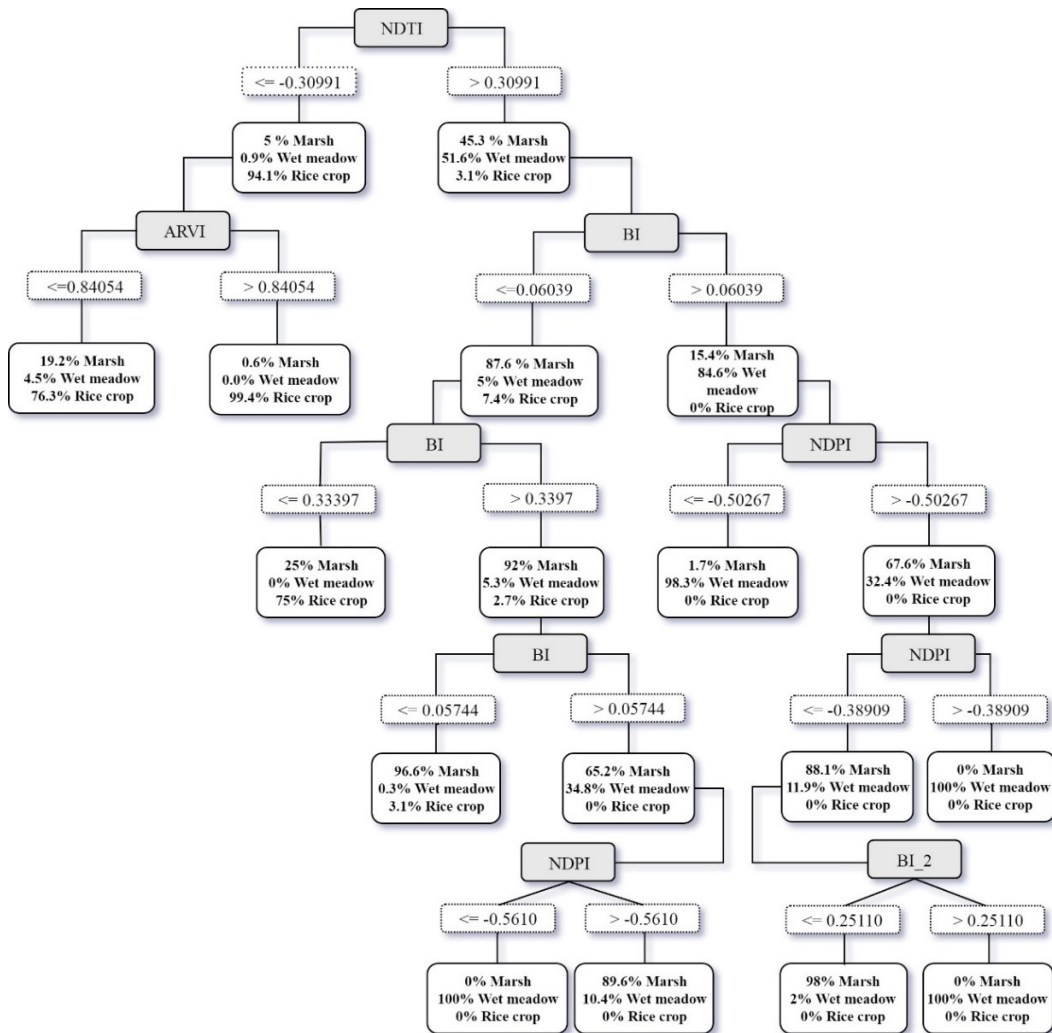


Figure 3. Classification and regression trees (CART) method decision tree (DT) for the present study.

that this index is reliable to classify rice cultivation areas since 98.5% of ARVI values higher than 0.84054 were categorized as rice crops.

The NDTI values higher than -0.31 classified 45.3% of the samples as SIMA and they were automatically associated with BI_1 (brightness index) (Escadafal, 1989). The BI showed to be adequate to classify marshes since 87.6% of the BI samples with values smaller than 0.06 were categorized as marsh areas. It is also important to note that the NDPI values higher than -0.56 classified 89.6% of the samples as marsh areas and the BI_2 values

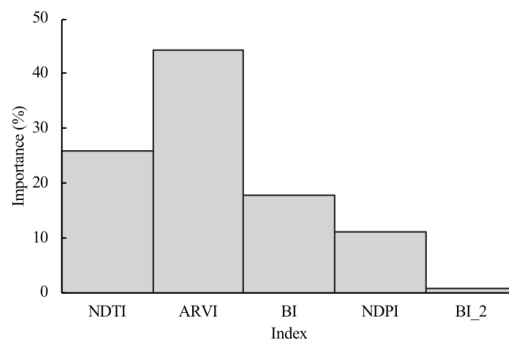


Figure 4. Indexes importance in the Decision Tree (DT) classification.

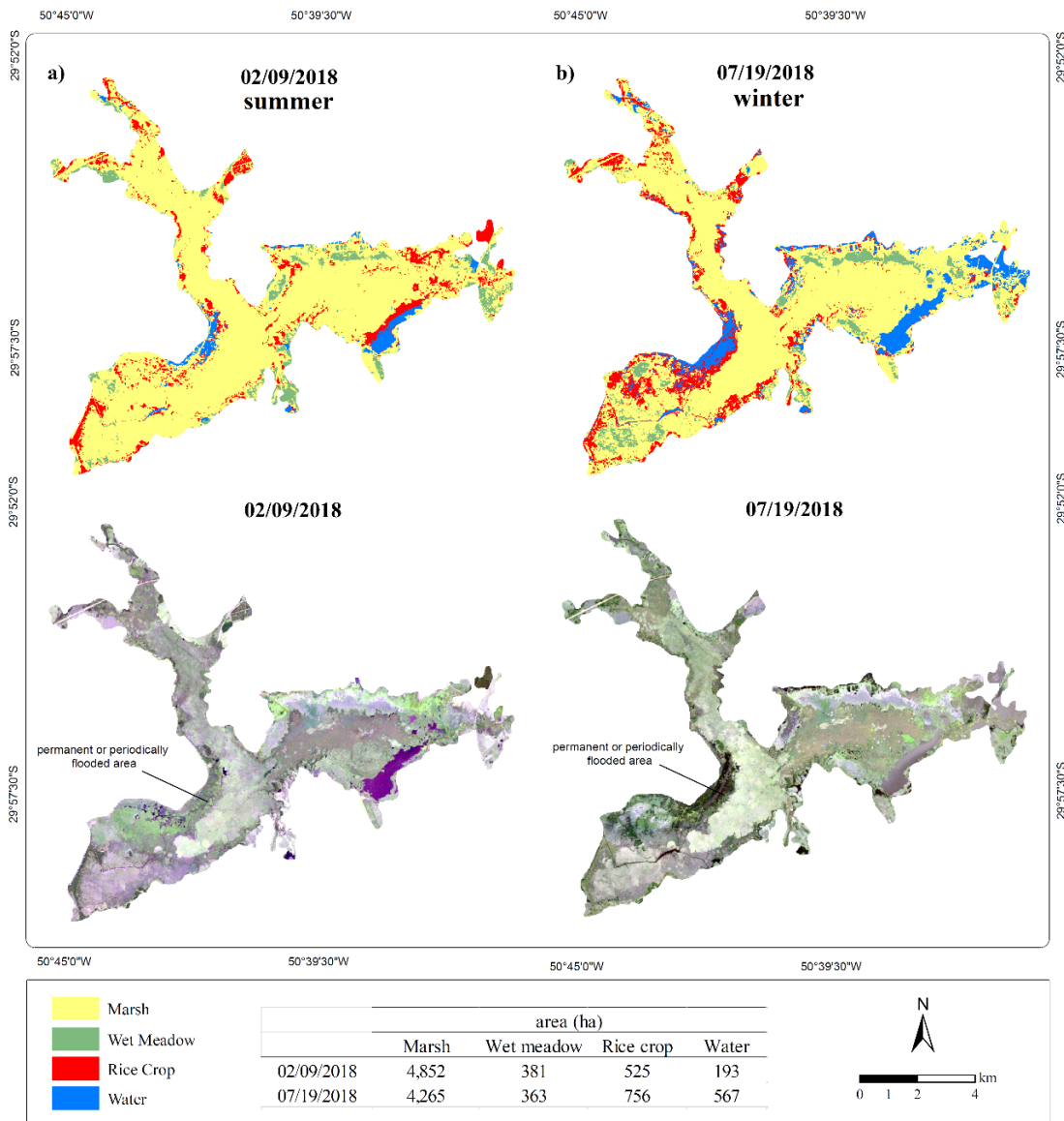


Figure 5. Classification and regression trees (CART) method results for the BG small inner marsh (SIM) area during the Summer (a) and Winter (b).

smaller than 0.25 classified 98% of the samples as marsh areas.

The relevant indexes for the DT creation using the CART method are showed in Figure 4. The most important index was ARVI (44% of total relevance) followed by NDTI, BI, NDPI and BI_2, with 25.9%, 17.7%, 11.1% and 0.8% total relevance, respectively. ARVI presented the best results to classify rice crops while NDTI, BI,

NDPI and BI_2 presented the best results to classify marsh areas.

The classification indexes relevance is related to the minimum impurity reduction required to divide a node, which means that higher values tend to produce trees with fewer nodes. This fact was noticed in both ARVI and NDTI, which created only one node each. The BI_2 is an exception

Table 3. Validation samples confusion matrix.

Classification 1 (Summer) – 02/09/2018				
	SIMA	WM	RC	UA (%)
SIMA	512	9	40	91.3
WM	8	595	6	97.7
RC	12	0	628	98.1
PA (%)	96.2	98.5	93.2	-
PC (%)	95.9			
Classification 2 (Winter) – 07/19/2018				
	SIMA	WM	RC	UA (%)
SIMA	455	69	37	81.1
WM	87	477	30	80.3
RC	78	88	440	72.6
PA (%)	73.3	75.2	86.7	-
PC (%)	77.9			

because it is in the last tree level characterizing itself as a leaf.

3.3. Marsh Delimitation

The areas classified as marshes by the DT for Summer and Winter seasons are presented in Figure 5. The summer image presented the best classification results compared to the winter image. The areas classified as rice crops are found on the BG edges (Figure 5a). In the Winter image (Figure 5b), CART classified flooded areas erroneously as rice cultivation. This error is most likely associated to the image acquisition period given the fact that in February rice cultivation presents a spectral response related to grain ripening phenology. On the other hand, in July, there is fallow vegetation and higher amplitude in the water level oscillation with similar response to the marshes areas.

The DT classification results showed that the SIM class presents the lower UA. For the Summer image, the SIM samples used for validation presented a 91.3% UA, followed by WM areas with 97.7% UA. The RC areas presented the best UA for the Summer image, with 98.1%. For the Winter image, the SIM class presented the higher UA, 81.1%, followed by the WM and RC areas, with 80.3% and 72.6% UA, respectively.

4. Discussion

ARVI was successful for rice crop classification with up to 98.5% PC. However, for marsh areas this index did not perform well, classifying only

23.3% of the samples as marshes. For SIM, the best results were obtained by the NDTI, BI and NDPI indexes, respectively. NDTI and NDPI have been successfully applied for wetland mapping by several studies. Some examples are the studies developed by 1) Mondal and Bandyopadhyay (2014), which delimited wetlands based on turbidity by mixing NDTI and NDPI techniques; and 2) Sharma *et al.* (2014), which used NDTI and NDPI to understand vegetation patterns and water turbidity in wetlands.

NDTI and NDPI indexes were specifically developed for studies over wetlands and their reliability in the delimitation of these areas was expected (Sharma *et al.*, 2014). We also highlight the good performance obtained with the BI. This index represents the average sensitive brightness to the soil, which is highly correlated with the moisture and the salt at the surface. The BI was developed to explore the soil surface characterization, mainly in arid environments, where vegetation is scarce and not green (Escadafal, 1989).

The hydromorphic soils presence in the study area, which is characterized by a high content of organic matter, allowed the BI application for marshes delimitation. This is discussed by Kandus *et al.* (2008), highlighting the importance of the soil taxonomic classification for wetlands delimitation. The marshes delimitation from the hydromorphic soils is also discussed by (Maltchik *et al.*, 2004). For these authors, the hydromorphic soils must be used as an environmental attribute in marshes delimitation in addition to the hydrological regime and aquatic vegetation patterns.

Our findings showed that the classification results for the Summer image presented a higher PC than the Winter image. This fact is most likely be related to seasonality of the flood pulses and vegetation patterns in the BG (Belloli, 2016; Simioni *et al.*, 2017).

5. Conclusions

The SIM areas delimitation remains a challenge for the scientific community considering that these wetlands present their own dynamics, with different aquatic vegetation types adapted to water level oscillations.

Our results showed that remote sensing indexes, although not developed specifically for wetland delimitation, present satisfactory results in order to classify these ecosystems. The indexes that showed to be more useful for marshes classification by DT techniques in the study area were NDTI, BI, NDPI and BI₂, with 25.9%, 17.7%, 11.1% and 0.8%, respectively. In general, the PC found was 95.9% and 77.9% for the Summer and Winter images respectively. We hypothesize that this significant PC variation is related to the rice-planting period in the Summer and/or to the water level oscillation period in the Winter.

For future studies, we recommend the use of active remote sensors (e.g., radar) and soil maps in addition to the remote sensing spectral indexes in order to obtain better results in the delimitation of small inner marsh areas.

Acknowledgment

João Paulo Delapasse Simioni thanks the CAPES agency for providing a doctoral fellowship. The authors acknowledge the Center for Remote Sensing and Meteorology (CEPSRM) at the Federal University of Rio Grande do Sul (UFRGS) for the support provided for this research.

References

Artigas, F. J., Yang, J. 2006. Spectral discrimination of marsh vegetation types in the New Jersey Meadowlands, USA. *Wetlands*, 26(1), 271. [https://doi.org/10.1672/0277-5212\(2006\)26\[271:sdovmt\]2.0.co;2](https://doi.org/10.1672/0277-5212(2006)26[271:sdovmt]2.0.co;2)

Belloli, T. F. 2016. *Environmental Impacts Due to Rice, Large Banhado Environmental Protection Area - RS*. Federal University of Rio Grande do Sul. Retrieved from <https://www.lume.ufrgs.br/bitstream/handle/10183/158968/001023034.pdf?sequence=1>

Belluco, E., Camuffo, M., Ferrari, S., Modenese, L., Silvestri, S., Marani, A., Marani, M. 2006. Mapping salt-marsh vegetation by multispectral and hyperspectral remote sensing. *Remote Sensing of Environment*, 105(1), 54-67. <https://doi.org/10.1016/j.rse.2006.06.006>

Canadian Wetland Inventory Technical Group. 2016. *Canada Wetland Inventory (Data Model)*. Stonewall. Retrieved from http://www.ducks.ca/assets/2017/01/CWIDMv7_01_E.pdf

Clevers, J. G. P. W., Leeuwen, H. J. C. Van, Sensing, R., Verhoef, W. 1989. Estimating apar by means of vegetation indeces: a sensitivity analysis. *XXIX ISPRS Congress Technical Commission VII: Interpretation of Photographic and Remote Sensing Data*, 691-698.

Congalton, R. G. 1991. A review of assessing the accuracy of classifications of remotely sensed data. *Remote Sensing of Environment*, 37(1), 35-46. [https://doi.org/10.1016/0034-4257\(91\)90048-B](https://doi.org/10.1016/0034-4257(91)90048-B)

Deering, D. W. 1975. Measuring forage production of grazing units from Landsat MSS data. *Proceedings of 10th International Symposium on Remote Sensing of Environment*, 1975, 1169-1178.

Delegido, J., Verrelst, J., Alonso, L., Moreno, J. 2011. Evaluation of sentinel-2 red-edge bands for empirical estimation of green LAI and chlorophyll content. *Sensors*, 11(7), 7063-7081. <https://doi.org/10.3390/s110707063>

Di Vittorio, C. A., Georgakakos, A. P. 2018. Land cover classification and wetland inundation mapping using MODIS. *Remote Sensing of Environment*, 204, 1-17. <https://doi.org/10.1016/j.rse.2017.11.001>

Dong, Z., Wang, Z., Liu, D., Song, K., Li, L., Jia, M., Ding, Z. 2014. Mapping Wetland Areas Using Landsat-Derived NDVI and LSWI: A Case Study of West Songnen Plain, Northeast China. *Journal of the Indian Society of Remote Sensing*, 42(3), 569-576. <https://doi.org/10.1007/s12524-013-0357-1>

Dvoretz, D., Davis, C., Papeş, M. 2016. Mapping and Hydrologic Attribution of Temporary Wetlands Using Recurrent Landsat Imagery. *Wetlands*, 36(3), 431-443. <https://doi.org/10.1007/s13157-016-0752-9>

Environmental Protection Agency. 2001. *Functions and Values of Wetlands*. Watershed Academy Web. Washington. Retrieved from <https://www.epa.gov/wetlandsfunctionsvalues>

- Escadafal, R. 1989. Remote sensing of arid soil surface color with Landsat thematic mapper. *Advances in Space Research*, 9(1), 159-163. [https://doi.org/10.1016/0273-1177\(89\)90481-X](https://doi.org/10.1016/0273-1177(89)90481-X)
- Etchelar, C. B. 2017. *Erosive Processes in Wetlands*. Rio Grande do Sul Federal University. Retrieved from <https://www.lume.ufrgs.br/bitstream/handle/10183/171041/001054625.pdf?sequence=1>
- Fariña, J. M., He, Q., Silliman, B. R., Bertness, M. D. 2017. Biogeography of salt marsh plant zonation on the Pacific coast of South America. *Journal of Biogeography*, 12, 238-247. <https://doi.org/10.1111/jbi.13109>
- Fluet-Chouinard, E., Lehner, B., Rebelo, L. M., Papa, F., Hamilton, S. K. 2015. Development of a global inundation map at high spatial resolution from topographic downscaling of coarse-scale remote sensing data. *Remote Sensing of Environment*, 158, 348-361. <https://doi.org/10.1016/j.rse.2014.10.015>
- Friedl, M.A. M. A., Brodley, C. E. C. E. 1997. Decision tree classification of land cover from remotely sensed data. *Remote Sensing of Environment*, 61(3), 399-409. [https://doi.org/10.1016/S0034-4257\(97\)00049-7](https://doi.org/10.1016/S0034-4257(97)00049-7)
- Gao, B. C. 1996. NDWI - A normalized difference water index for remote sensing of vegetation liquid water from space. *Remote Sensing of Environment*, 58(3), 257-266. [https://doi.org/10.1016/S0034-4257\(96\)00067-3](https://doi.org/10.1016/S0034-4257(96)00067-3)
- Gedan, K. B., Crain, C. M., Bertness, M. D. 2009. Small-mammal herbivore control of secondary succession in New-England tidal marshes. *Ecology*, 90(2), 430-440. <https://doi.org/10.1890/08-0417.1>
- Gitelson, A. A., Kaufman, Y. J., Merzlyak, M. N. 1996. Use of a green channel in remote sensing of global vegetation from EOS-MODIS. *Remote Sensing of Environment*, 58(3), 289-298. [https://doi.org/10.1016/S0034-4257\(96\)00072-7](https://doi.org/10.1016/S0034-4257(96)00072-7)
- Huete, A. R. 1988. A soil-adjusted vegetation index (SAVI). *Remote Sensing of Environment*, 25(3), 295-309. [https://doi.org/10.1016/0034-4257\(88\)90106-X](https://doi.org/10.1016/0034-4257(88)90106-X)
- Jensen, J. R. 2007. *Remote sensing of the environment : an earth resource perspective*. Pearson Prentice Hall.
- Judd, C., Steinberg, S., Shaughnessy, F., Crawford, G. 2007. Mapping salt marsh vegetation using aerial hyperspectral imagery and linear unmixing in Humboldt Bay, California. *Wetlands*, 27(4), 1144-1152. [https://doi.org/10.1672/0277-5212\(2007\)27\[1144:mismvua\]2.0.co;2](https://doi.org/10.1672/0277-5212(2007)27[1144:mismvua]2.0.co;2)
- Junk, 2013. *Definição e Classificação das Áreas Úmidas (AUs) Brasileiras* : Base Científica para uma Nova Política de Proteção e Manejo Sustentável Prefácio : Lista dos autores e suas instituições : Centro de Pesquisa Do Pantanal, Brazil.
- Junk, W. J., Bayley, P. B., Sparks, R. E. 1989. The Flood Pulse Concept in River-Floodplain Systems. *International Large River Symposium*.
- Junk, W. J., Piedade, M. F. 2015. Áreas Úmidas (AUs) Brasileiras: Avanços e Conquistas Recentes. *Boletim Ablimno*, 41(2), 20-24.
- Junk, W. J., Piedade, M. T. F., Lourival, R., Wittmann, F., Kandus, P., Lacerda, L. D., Agostinho, A. A. 2014. Brazilian wetlands: Their definition, delineation, and classification for research, sustainable management, and protection. *Aquatic Conservation: Marine and Freshwater Ecosystems*, 24(1), 5-22. <https://doi.org/10.1002/aqc.2386>
- Kandus, P., Minotti, P., Malvárez, A. I. 2008. Distribution of wetlands in Argentina estimated from soil charts. *Acta Scientiarum - Biological Sciences*, 30(4), 403-409. <https://doi.org/10.4025/actasciobiolsci.v30i4.5870>
- Kaplan, G., Avdan, U. 2017. Mapping and Monitoring Wetlands Using SENTINEL 2 Satellite Imagery. *ISPRS Annals of Photogrammetry, Remote Sensing and Spatial Information Sciences, IV*, 271-277. <https://doi.org/10.5194/isprs-annals-IV-4-W4-271-2017>
- Kaplan, G., Avdan, U. 2017. Wetland Mapping Using Sentinel 1 SAR Data. In Suha Ozden, R. Cengiz Akbulak, Cuneyt Erenoglu, Ozgur Karaca, Faize Saris, & Mustafa Avcioglu (Eds.), *International Symposium on GIS Applications in Geography & Geosciences*.
- Kaufman, Y., Tanre, D. 1992. 1992. Atmospherically resistant vegetation index (ARVI) for EOS-MODIS. *IEEE Transactions on Geoscience and Remote Sensing*, 30(2). <https://doi.org/10.1109/36.134076>
- Kulawardhana, R. W., Thenkabail, P. S., Vithanage, J., Biradar, C., Islam, M. A. a, Gunasinghe, S., Alankara, R. 2007. Evaluation of the wetland mapping methods using Landsat ETM+ and SRTM data. *Journal of Spatial Hydrology*, 7(2), 62-96. <https://doi.org/10.1017/CBO9780511806049>
- Lacaux, J. P., Tourre, Y. M., Vignolles, C., Ndione, J. A., Lafaye, M. 2007. Classification of ponds from high-spatial resolution remote sensing: Application to Rift Valley Fever epidemics in Senegal. *Remote Sensing of Environment*, 106(1), 66-74. <https://doi.org/10.1016/j.rse.2006.07.012>
- Leite, M. G., Guasselli, L. A. 2013. Spatio-temporal dynamics of aquatic macrophytes in Banhado Grande, Gravataí River basin,. *Para Onde!?*, 7(1), 17-24.

- Liu, L., Liu, Y. H., Liu, C. X., Wang, Z., Dong, J., Zhu, G. F., Huang, X. 2013. Potential effect and accumulation of veterinary antibiotics in *Phragmites australis* under hydroponic conditions. *Ecological Engineering*, 53, 138-143. <https://doi.org/10.1016/j.ecoleng.2012.12.033>
- Mahdavi, S., Salehi, B., Amani, M., Granger, J. E., Brisco, B., Huang, W., Hanson, A. 2017. Object-Based Classification of Wetlands in Newfoundland and Labrador Using Multi-Temporal PolSAR Data. *Canadian Journal of Remote Sensing*, 43(5), 432-450. <https://doi.org/10.1080/07038992.2017.1342206>
- Maltchik, L., Rolon, A. S., Guadagnin, D. L., Stenert, C. 2004. Wetlands of Rio Grande do Sul, Brazil: a classification with emphasis on plant communities. *Acta Limnol. Bras*, 16(2), 137-151.
- Mao, R., Ye, S.-Y., Zhang, X.-H. 2018. Soil-Aggregate-Associated Organic Carbon Along Vegetation Zones in Tidal Salt Marshes in the Liaohe Delta. *CLEAN - Soil, Air, Water*, 1-7. <https://doi.org/10.1002/clen.201800049>
- McFeeters, S. K. 1996. The use of the Normalized Difference Water Index (NDWI) in the delineation of open water features. *International Journal of Remote Sensing*, 17(7), 1425-1432. <https://doi.org/10.1080/01431169608948714>
- Mcowen, C. J., Weatherdon, L. V., Bochove, J.-W. Van, Sullivan, E., Blyth, S., Zockler, C., Fletcher, S. 2017. A global map of saltmarshes. *Biodiversity Data Journal*, 5(5), e11764. <https://doi.org/10.3897/BDJ.5.e11764>
- Miranda, C. de S., Paranho Filho, A. C., Pott, A. 2018. Changes in vegetation cover of the Pantanal wetland detected by vegetation index: a strategy for conservation. *Biota Neotropica*, 18(1), 1-6. <https://doi.org/10.1590/1676-0611-bn-2016-0297>
- Mondal, I., Bandyopadhyay, J. 2014. Coastal Wetland Modeling Using Geoinformatics Technology of Namkhana Island, South 24 Parganas, WB, India. *Open Access Library Journal*, 975, 1-17. <https://doi.org/10.4236/oalib.1100975>
- Nielsen, S. 1994. Geomorfologia da bacia do rio Gravataí-RS. In *Bacia do rio Gravataí-RS: informações básicas para a gestão territorial* (pp. 1-18). Porto Alegre: Proteger.
- Nunes da Cunha, C., Piedade, M. T. F., Junk, W. J. 2015. *Classificação e Delineamento das Áreas Úmidas Brasileiras e de seus Macrohabitats*. EdUFMT (Vol. 1). Cuiaba. <https://doi.org/10.1017/CBO9781107415324.004>
- Pearson, R. L., Miller, L. D. 1972. Remote Mapping of Standing Crop Biomass for Estimation of the Productivity of the Shortgrass Prairie. *Remote Sensing of Environment*, 8, 1355-1365.
- Pontius, R. G., Millones, M. 2011. Death to Kappa: Birth of quantity disagreement and allocation disagreement for accuracy assessment. *International Journal of Remote Sensing*, 32(15), 4407-4429. <https://doi.org/10.1080/01431161.2011.552923>
- Qi, J., Chehbouni, A., Huete, A. R., Kerr, Y. H., Sorooshian, S. 1994. A modified soil adjusted vegetation index. *Remote Sensing of Environment*, 48(2), 119-126. [https://doi.org/10.1016/0034-4257\(94\)90134-1](https://doi.org/10.1016/0034-4257(94)90134-1)
- Ramos, R. A., Pasqualetto, A. I., Balbuena, R. A., Quadros, E. L. L. de, Neves, D. D. das. 2014. Mapeamento e diagnóstico de áreas úmidas no Rio Grande do Sul, com o uso de ferramentas de geoprocessamento. In *Anais do Simposio de Áreas Protegidas* (pp. 17-21). Viçosa.
- Ramsar. 2002. *A Framework for Wetland Inventory*. 8th Meeting of the Conference of the Contracting Parties to the Convention on Wetlands. Valencia. Retrieved from <http://archive.ramsar.org/pdf/inventory-framework-2002.pdf>
- Richardson, A. J., Wiegand, C. L. 1977. Distinguishing vegetation from soil background information. *Photogrammetric Engineering and Remote Sensing*, 43(12), 1541-1552.
- Rossato, M. S. 2011. *Os climas do Rio Grande do Sul: variabilidade, tendências e tipologia*. Universidade Federal do Rio Grande do Sul.
- Rouse, J. W., Hass, R. H., Schell, J. A., Deering, D. W. 1973. Monitoring vegetation systems in the great plains with ERTS. *Third Earth Resources Technology Satellite (ERTS) Symposium*, 1, 309-317. <https://doi.org/citeulike-article-id:12009708>
- Ruiz, L. F. C., Caten, A. ten, Dalmolin, R. S. D. 2014. Árvore de decisão e a densidade mínima de amostras no mapeamento da cobertura da terra. *Ciência Rural*, 44(6), 1001-1007. <https://doi.org/10.1590/S0103-84782014000600008>
- Sakané, N., Alvarez, M., Becker, M., Böhme, B., Handa, C., Kamiri, H. W., Langensiepen, M., Menz, G., Misana, S., Mogha, N. G., Mösele, B. M., Mwita, E. J., Oyieke, H. A., Van Wijk, M. T. 2011. Classification, characterisation, and use of small wetlands in East Africa. *Wetlands*, 31, 1103. <https://doi.org/10.1007/s13157-011-0221-4>
- Sharma, A., Panigrahy, S., Singh, T. S., Patel, J. G., Tanwar, H. 2014. Wetland Information System Using Remote Sensing and GIS in Himachal Pradesh, India. *Asian Journal of Geoinformatics*, 14(4), 13-22.

- Sharpe, P. J., Kneipp, G., Forget, A. 2016. Comparison of Alternative Approaches for Wetlands Mapping: A Case Study from three U.S. National Parks. *Wetlands*, 36(3), 547-556. <https://doi.org/10.1007/s13157-016-0764-5>
- Silva, R. C. da. 2016. *Estudo da dinâmica da fragilidade ambiental na Bacia Hidrográfica do Rio Gravataí*, RS. Universidade Federal da Bahia.
- Simioni, J. P. D., Guasselli, L. A., Etchelar, C. B. 2017. Connectivity among Wetlands of EPA of Banhado Grande, RS Conetividade entre Áreas Úmidas, APA do Banhado Grande, RS. *Brazilian Journal of Water Resources*, 22(15). <https://doi.org/10.1590/2318-0331.011716096>
- Stefano, L. de. 2003. *WWF 's Water and Wetland Index Summary of Water Framework Directive results*. WWF European Living Waters Programme c/o. San Francisco.
- Subramaniam, S., Saxena, M. 2011. Automated algorithm for extraction of wetlands from IRS resourcesat LISS III data. In *International Archives of the Photogrammetry, Remote Sensing and Spatial Information Sciences* (pp. 193-198). Bhopal.
- Teixeira, S. G. 2011. *Radar de abertura sintética aplicado ao mapeamento e reconhecimento de zonas úmidas costeiras*. Universidade Federal do Pará.
- Visser, J. M., Sasser, C. E. 1999. Marsh Vegetation of the Mississippi River Deltaic Plain. *Estuaries*, 21(4B), 818-828.
- Walsh, N., Bhattasali, N., Chay, F. 2014. Mapping Tidal Salt Marshes.
- White, D. C., Lewis, M. M., Green, G., Gotch, T. B. 2016. A generalizable NDVI-based wetland delineation indicator for remote monitoring of groundwater flows in the Australian Great Artesian Basin. *Ecological Indicators*, 60, 1309-1320. <https://doi.org/10.1016/j.ecolind.2015.01.032>
- Xu, H. 2006. Modification of normalised difference water index (NDWI) to enhance open water features in remotely sensed imagery. *International Journal of Remote Sensing*, 27(14), 3025-3033. <https://doi.org/10.1080/01431160600589179>
- Yan, D., Wünnemann, B., Hu, Y., Frenzel, P., Zhang, Y., Chen, K. 2017. Wetland evolution in the Qinghai Lake area, China, in response to hydrodynamic and eolian processes during the past 1100 years. *Quaternary Science Reviews*, 162, 42-59.
- Zhou, Q., Jing, Z., Jiang, S. 2003. Remote sensing image fusion for different spectral and spatial resolutions with bilinear resampling wavelet transform. In *Proceedings of the 2003 IEEE International Conference on Intelligent Transportation Systems 2*, 1206-1213. Shanghai: IEEE. <https://doi.org/10.1109/ITSC.2003.1252676>